

An Almost Optimal Bound on the Number of Intersections of Two Simple Polygons

Eyal Ackerman

Department of Mathematics, Physics, and Computer Science, University of Haifa at Oranim,
Tivon 36006, Israel
ackerman@sci.haifa.ac.il

Balázs Keszegh 

Alfréd Rényi Institute of Mathematics, H-1053 Budapest, Hungary
MTA-ELTE Lendület Combinatorial Geometry Research Group, Budapest, Hungary
keszegh@renyi.hu

Günter Rote 

Department of Computer Science, Freie Universität Berlin, Takustr. 9, 14195 Berlin, Germany
rote@inf.fu-berlin.de

Abstract

What is the maximum number of intersections of the boundaries of a simple m -gon and a simple n -gon, assuming general position? This is a basic question in combinatorial geometry, and the answer is easy if at least one of m and n is even. If both m and n are odd, the best known construction has $mn - (m + n) + 3$ intersections, and it is conjectured that this is the maximum. However, the best known upper bound is only $mn - (m + \lceil \frac{n}{6} \rceil)$, for $m \geq n$. We prove a new upper bound of $mn - (m + n) + C$ for some constant C , which is optimal apart from the value of C .

2012 ACM Subject Classification Theory of computation → Computational geometry; Mathematics of computing → Combinatoric problems

Keywords and phrases Simple polygon, Ramsey theory, combinatorial geometry

Digital Object Identifier 10.4230/LIPIcs.SoCG.2020.1

Related Version A slightly expanded version is available at <http://arxiv.org/abs/2002.05680>.

Funding *Eyal Ackerman*: The main part of this work was performed during a visit to Freie Universität Berlin which was supported by the Freie Universität Alumni Program.

Balázs Keszegh: Research supported by the Lendület program of the Hungarian Academy of Sciences (MTA), under the grant LP2017-19/2017 and by the National Research, Development and Innovation Office – NKFIH under the grant K 116769.

Acknowledgements We thank the reviewers for helpful suggestions.

1 Introduction

To determine the union of two or more geometric objects in the plane is one of the basic computational geometric problems. In strong relation to that, determining the maximum complexity of the union of two or more geometric objects is a basic extremal geometric problem. We study this problem when the two objects are simple polygons.

Let P and Q be two simple polygons with m and n sides, respectively, where $m, n \geq 3$. For simplicity we always assume general position in the sense that no three vertices (of P and Q combined) lie on a line and no two sides (of P and Q combined) are parallel. We are interested in the maximum number of intersections of the boundaries of P and Q .

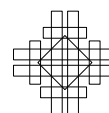
This problem was first studied in 1993 by Dillencourt, Mount, and Saalfeld [2]. The cases when m or n is even are solved there. If m and n are both even, then every pair of sides may cross and so the answer is mn . Figure 1a shows one of many ways to achieve this number.

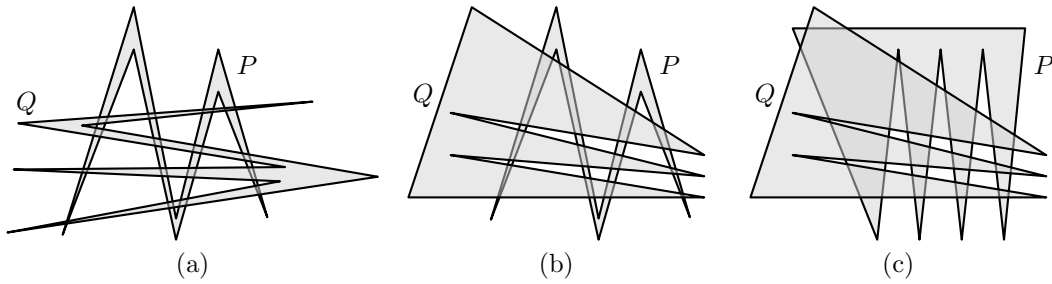


© Eyal Ackerman, Balázs Keszegh, and Günter Rote;
licensed under Creative Commons License CC-BY
36th International Symposium on Computational Geometry (SoCG 2020).
Editors: Sergio Cabello and Danny Z. Chen; Article No. 1; pp. 1:1–1:18
Leibniz International Proceedings in Informatics



Schloss Dagstuhl – Leibniz-Zentrum für Informatik, Dagstuhl Publishing, Germany





■ **Figure 1** (a) Optimal construction for $m = n = 8$, with $8 \times 8 = 64$ intersections. (b) Optimal construction for $m = 8$, $n = 7$, with $8 \times 6 = 48$ intersections. (c) Lower-bound construction for $m = 9$, $n = 7$. There are $8 \times 6 + 2 = 50$ intersections.

If one polygon, say Q , has an odd number n of sides, no line segment s can be intersected n times by Q , because otherwise each side of Q would have to flip from one side of s to the other side. Thus, each side of the m -gon P is intersected at most $n - 1$ times, for a total of at most $mn - m$ intersections. It is easy to see that this bound is tight when P has an even number of sides, see Figure 1b.

When both m and n are odd, the situation is more difficult; the bound that is obtained by the above argument remains at $mn - \max\{m, n\}$, because the set of m intersections that are necessarily “missing” due to the odd parity of n might conceivably overlap with the n intersections that are “missing” due to the odd parity of m . However, the best known family of examples gives only $mn - (m + n) + 3 = (m - 1)(n - 1) + 2$ intersection points, see Figure 1c. Note that in Figure 1, all vertices of the polygons contribute to the boundary of the union of the polygon areas.

► **Conjecture 1.** *Let P and Q be simple polygons with m and n sides, respectively, such that $m, n \geq 3$ are odd numbers. Then there are at most $mn - (m + n) + 3$ intersection points between sides of P and sides of Q .*

In [2] an unrecoverable error appears in a claimed proof of Conjecture 1. Another attempted proof [5] also turned out to have a fault. The only correct improvement over the trivial upper bound is an upper bound of $mn - (m + \lceil \frac{n}{6} \rceil)$ for $m \geq n$, due to Černý, Kára, Král', Podbrdský, Sotáková, and Šámal [1]. We will briefly discuss their proof in Section 2.

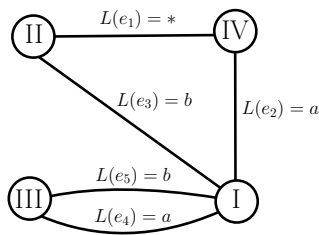
We improve the upper bound to $mn - (m + n) + O(1)$, which is optimal apart from an additional constant:

► **Theorem 1.** *There is an absolute constant C such that the following holds. Suppose that P and Q are simple polygons with m and n sides, respectively, such that m and n are odd numbers. Then there are at least $m + n - C$ pairs of a side of P and a side of Q that do not intersect. Hence, there are at most $mn - (m + n) + C$ intersections.*

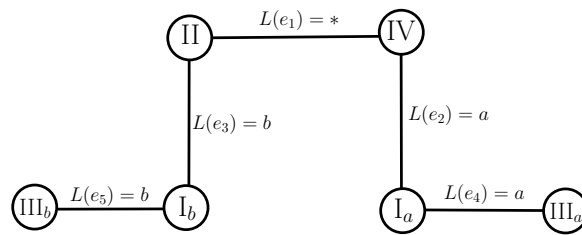
The value of the constant C that we obtain in our proof is around $2^{2^{67}}$. We did not make a large effort to optimize this value, and obviously, there is ample space for improvement.

2 Overview of the proof

First we establish the crucial statement that the odd parity of m and n allows us to *associate* to any two consecutive sides of one polygon a pair of consecutive sides of the other polygon with a restricted intersection pattern among the four involved sides (Lemma 5 and Figure 5). This is the only place where we use the odd parity of the polygons.



■ **Figure 2** The edge-labeled multigraph G_0 in Proposition 2.



■ **Figure 3** The unfolded graph G'_0 .

A simple observation (Observation 3) relates the bound on C in Theorem 1 to the number of connected components of the bipartite “disjointness graph” between the polygon sides of P and Q . Our goal is therefore to show that there are few connected components.

We proceed to consider *two* pairs of associated pairs of sides (4 consecutive pairs with 8 sides in total). Unless they form a special structure, they cannot belong to four different connected components (Lemma 7). (Four is the maximum number of components that they could conceivably have.) The proof involves a case distinction with a moderate amount of cases. This structural statement allows us to reduce the bound on the number of components by a constant factor, and thereby, we can already improve the best previous result on the number of intersections (Proposition 9 in Section 6).

Finally, to get a constant bound on the number of components, our strategy is to use Ramsey-theoretic arguments like the Erdős–Szekeres Theorem on caps and cups or the pigeonhole principle (see Section 7) in order to impose additional structure on the configurations that we have to analyze. This is the place in the argument where we give up control over the constant C in exchange for useful properties that allow us to derive a contradiction. This eventually boils down again to a moderate number of cases (Section 8.2).

By contrast, the proof of the bound $mn - (m + \lceil \frac{n}{6} \rceil)$ for $m \geq n$ proceeds more locally. The core of the argument [1, Lemma 3], which is proved by case distinction, is that it is impossible to have 6 consecutive sides of one polygon together with 6 distinct sides of the other polygon forming a perfect matching in the disjointness graph. This statement is used to bound the number of components of the disjointness graph. (Lemma 8 below uses a similar argument.)

3 An auxiliary lemma on closed odd walks

We begin with the following seemingly unrelated claim concerning a specific small edge-labeled multigraph. Let $G_0 = (V_0, E_0)$ be the undirected multigraph shown in Figure 2. It has four nodes $V_0 = \{I, II, III, IV\}$ and five edges $E_0 = \{e_1 = \{II, IV\}, e_2 = \{I, IV\}, e_3 = \{I, II\}, e_4 = \{I, III\}, e_5 = \{I, III\}\}$. Every edge $e_i \in E_0$ has a label $L(e_i) \in \{a, b, *\}$ as follows: $L(e_1) = *$, $L(e_2) = L(e_4) = a$, $L(e_3) = L(e_5) = b$.

► **Proposition 2.** *If W is a closed walk in G_0 of odd length, then W contains two cyclically consecutive edges of labels a and b .*

Proof. Suppose for contradiction that W does not contain two consecutive edges of labels a and b . Since W cannot switch between the a -edges and the b -edges in I or III, we can split I (resp., III) into two nodes I_a and I_b (resp., III_a and III_b) such that every a -labeled edge that is incident to I (resp., III) in G_0 becomes incident to I_a (resp., III_a) and every b -labeled edge

that is incident to I (resp., III) in G_0 becomes incident to I_b (resp., III_b). In the resulting graph G'_0 , which is shown in Figure 3, we can find a closed walk W' that corresponds to W and that uses the edges with the same name as W . Since G'_0 is a path, every closed walk has even length. Thus, W cannot have odd length. ◀

4 General assumptions and notations

Let P and Q be two simple polygons with sides p_0, p_1, \dots, p_{m-1} and q_0, q_1, \dots, q_{n-1} . We assume that $m \geq 3$ and $n \geq 3$ are odd numbers. Addition and subtraction of indices is modulo m or n , respectively. We consider the sides p_i and q_j as closed line segments. The condition that the polygon P is simple means that its edges are pairwise disjoint except for the unavoidable common endpoints between *consecutive* sides p_i and p_{i+1} . Throughout this paper, unless stated otherwise, we regard a polygon as a piecewise linear closed curve, and we disregard the region that it encloses. Thus, by intersections between P and Q , we mean intersection points between the polygon *boundaries*.

As mentioned, we assume that the vertices of P and Q are in general position (no three of them on a line), and so every intersection point between P and Q is an interior point of two polygon sides.

The disjointness graph. As in [1], our basic tool of analysis is the *disjointness graph* of P and Q , which we denote by $G^D = (V^D, E^D)$. (Its original name in [1] is *non-intersection graph*.) It is a bipartite graph with node set $V^D = \{p_0, p_1, \dots, p_{m-1}\} \cup \{q_0, q_1, \dots, q_{n-1}\}$ and edge set $E^D = \{(p_i, q_j) \mid p_i \cap q_j = \emptyset\}$. (Since we are interested in the situation where almost all pairs of edges intersect, the disjointness graph is more useful than its more commonly used complement, the intersection graph.)

Our goal is to bound from above the number of connected components of G^D :

► **Observation 3.** *If G^D has at most C connected components, then G^D has at least $m+n-C$ edges. Thus, there are at least $m+n-C$ pairs of a side of P and a side of Q that do not intersect, and there are at most $mn - (m+n) + C$ crossings between P and Q .* ◀

Geometric notions. Let s and s' be two line segments. We denote by $\ell(s)$ the line through s and by $I(s, s')$ the intersection of $\ell(s)$ and $\ell(s')$ see Figure 4. We say that s and s' are *avoiding* if neither of them contains $I(s, s')$. (This requirement is stronger than just disjointness.) If s and s' are avoiding or share an endpoint, we denote by $\vec{r}_{s'}(s)$ the ray from $I(s, s')$ to infinity that contains s , and by $\vec{r}_s(s')$ the ray from $I(s, s')$ to infinity that contains s' . Moreover, we denote by $\text{Cone}(s, s')$ the convex cone with apex $I(s, s')$ between these two rays.

► **Observation 4.** *If a segment s'' that does not go through $I(s, s')$ has one of its endpoints in the interior of $\text{Cone}(s, s')$, then s'' cannot intersect both $\vec{r}_{s'}(s)$ and $\vec{r}_s(s')$. In particular, it cannot intersect both s and s' .* ◀

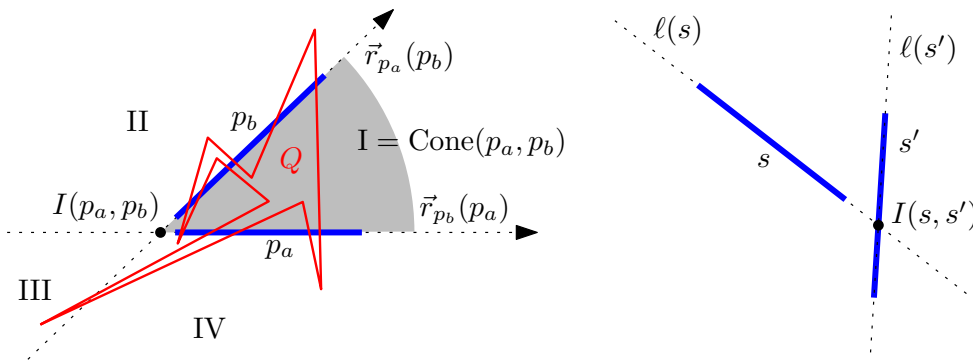
For a polygon side s of P or Q , $\text{CC}(s)$ denotes the connected component of the disjointness graph G^D to which s belongs.

4.1 Associated pairs of consecutive sides

► **Lemma 5.** *Let p_a and p_b be two sides of P that are either consecutive or avoiding such that $\text{CC}(p_a) \neq \text{CC}(p_b)$. Then there are two consecutive sides $q_i, q_{i\pm 1}$ of Q such that $(p_a, q_i), (p_b, q_{i\pm 1}) \in E^D$ and $(p_a, q_{i\pm 1}), (p_b, q_i) \notin E^D$. Furthermore, $I(p_a, p_b) \in \text{Cone}(q_i, q_{i\pm 1})$ or $I(q_i, q_{i\pm 1}) \in \text{Cone}(p_a, p_b)$.*

The sign “ \pm ” is needed since we do not know which of the consecutive sides intersects p_i and is disjoint from p_{i+1} .

Proof. We may assume without loss of generality that $I(p_a, p_b)$ is the origin, p_a lies on the positive x -axis and the interior of p_b is above the x -axis. The lines $\ell(p_a)$ and $\ell(p_b)$ partition the plane into four convex cones (“quadrants”). Denote them in counterclockwise order by I, II, III, IV, starting with $I = \text{Cone}(p_a, p_b)$, see Figure 4. Every side of Q must intersect p_a



■ **Figure 4** How an odd polygon Q can intersect two segments. The segments p_a and p_b are avoiding, whereas s and s' are disjoint but non-avoiding. In this situation, we say that s *stabs* s' .

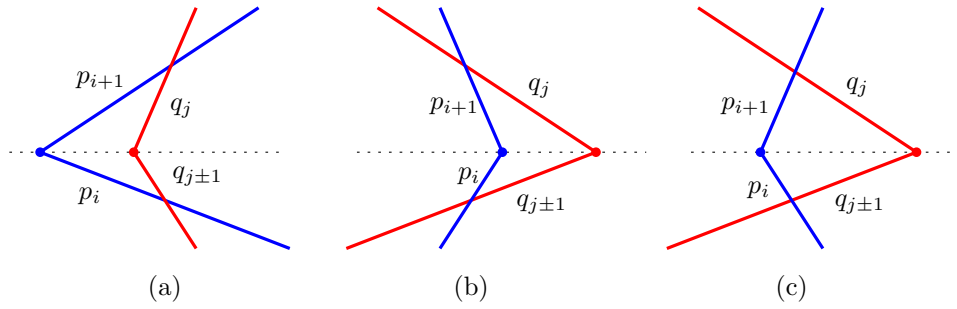
or p_b (maybe both), since $\text{CC}(p_a) \neq \text{CC}(p_b)$. One can now check that traversing the sides of Q in order generates a closed walk W in the graph G_0 of Figure 2. For example, a side of Q that we traverse from its endpoint in I to its endpoint in III and that intersects p_a corresponds to traversing the edge $e_4 = \{I, III\}$ from I to III, whose label is $L(e_4) = a$. We do not care which of p_a and p_b are crossed when we move between II and IV.

It follows from Proposition 2 that Q has two consecutive sides $q_i, q_{i\pm 1}$ such that q_i intersects p_b and does not intersect p_a , while $q_{i\pm 1}$ intersects p_a and does not intersect p_b . Hence, $(p_a, q_i), (p_b, q_{i\pm 1}) \in E^D$ and $(p_a, q_{i\pm 1}), (p_b, q_i) \notin E^D$. Furthermore, $I(q_i, q_{i\pm 1})$ must be either in I or III as these are the only nodes in G_0 that are incident both to an edge labeled a and an edge labeled b . In the latter case $I(p_a, p_b) \in \text{Cone}(q_i, q_{i\pm 1})$, and in the former case $I(q_i, q_{i\pm 1}) \in \text{Cone}(p_a, p_b)$. ◀

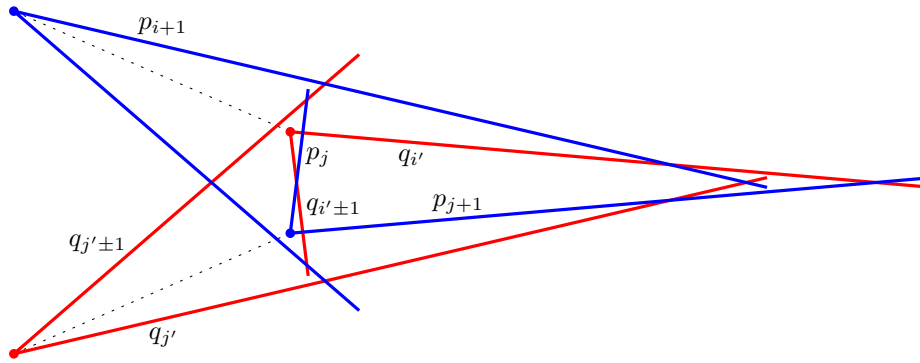
Let p_i, p_{i+1} be two sides of P such that $\text{CC}(p_i) \neq \text{CC}(p_{i+1})$. Then by Lemma 5 there are sides $q_j, q_{j\pm 1}$ of Q such that $(p_i, q_j), (p_{i+1}, q_{j\pm 1}) \in E^D$. We say that the pair $q_j, q_{j\pm 1}$ is *associated* to p_i, p_{i+1} . By Lemma 5 we have $I(q_j, q_{j\pm 1}) \in \text{Cone}(p_i, p_{i+1})$ or $I(p_i, p_{i+1}) \in \text{Cone}(q_j, q_{j\pm 1})$. If the first condition holds we say that p_i, p_{i+1} is *hooking* and $q_j, q_{j\pm 1}$ is *hooked*, see Figure 5. In the second case we say that p_i, p_{i+1} is *hooked* and $q_j, q_{j\pm 1}$ is *hooking*. Note that it is possible that a pair of consecutive sides is both hooking and hooked (with respect to two different pairs from the other polygon or even with respect to a single pair, as in Figure 5c).

▶ **Observation 6** (The Axis Property). *If the pair p_i, p_{i+1} and the pair $q_j, q_{j\pm 1}$ are associated such that $(p_i, q_j), (p_{i+1}, q_{j\pm 1}) \in E^D$, then the line through $I(p_i, p_{i+1})$ and $I(q_j, q_{j\pm 1})$ separates p_i and $q_{j\pm 1}$ on the one side from p_{i+1} and q_j on the other side.* ◀

We call this line the *axis* of the associated pairs. In our figures it appears as a dotted line when it is shown.



■ **Figure 5** Hooking and hooked pairs of consecutive sides. (a) The pair p_i, p_{i+1} is hooking and the associated pair $q_j, q_{j\pm 1}$ is hooked. (b) vice versa. (c) Both pairs are both hooking and hooked.



■ **Figure 6** The pair p_i, p_{i+1} is hooking with respect to the pair $q_{i'}, q_{i'\pm 1}$, and p_j, p_{j+1} is hooked with respect to $q_{j'}, q_{j'\pm 1}$.

5 The principal structure lemma about pairs of associated pairs

► **Lemma 7.** *Let $p_i, p_{i+1}, p_j, p_{j+1}$ be two pairs of consecutive sides of P that belong to four different connected components of G^D . Then it is impossible that both p_i, p_{i+1} and p_j, p_{j+1} are hooked or that both pairs are hooking.*

Figure 6 shows a scenario with four different components, together with the associated pairs of Q . The combinatorial structure of such a configuration is unique up to relabeling.

Proof. Suppose first that both pairs p_i, p_{i+1} and p_j, p_{j+1} , are hooking and let $q_{i'}, q_{i'\pm 1}$ and $q_{j'}, q_{j'\pm 1}$ be their associated (hooked) pairs such that: $(p_i, q_{i'}), (p_{i+1}, q_{i'\pm 1}) \in E^D$, $(p_j, q_{j'}), (p_{j+1}, q_{j'\pm 1}) \in E^D$, $I(q_{i'}, q_{i'\pm 1}) \in \text{Cone}(p_i, p_{i+1})$ and $I(q_{j'}, q_{j'\pm 1}) \in \text{Cone}(p_j, p_{j+1})$.

For better readability, we rename p_i, p_{i+1} and $q_{i'}, q_{i'\pm 1}$ as a, b and A, B , and we rename p_j, p_{j+1} and $q_{j'}, q_{j'\pm 1}$ as a', b' and A', B' . The small letters denote sides of P and the capital letters denote sides of Q . In the new notation, a, b are consecutive sides of P with an associated pair A, B of consecutive sides of Q , and a', b' are two other consecutive sides of P with an associated pair A', B' of consecutive sides of Q . The disjointness graph G^D contains the edges $(a, A), (b, B), (a', A'), (b', B')$. Since a, b, a', b' belong to different connected components of G^D , it follows that the nodes A, B, A', B' , to which they are connected, belong to the same four different connected components. There can be no more edges among these eight nodes, and they induce a matching in G^D . One can remember as a rule that every side of P intersects every side of Q among the eight involved sides, except when their names

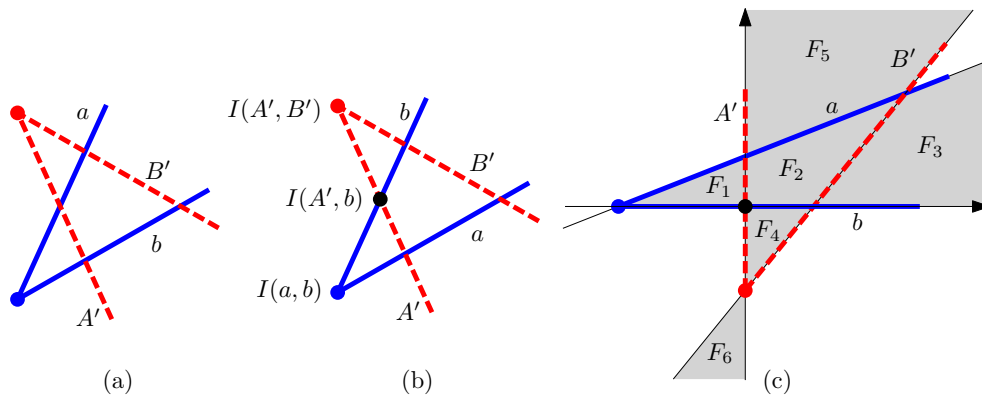


Figure 7 Normalizing the position of a, b, A', B' .

differ only in their capitalization. In particular, each of A' and B' intersects each of a and b and hence they must lie as in Figure 7a. To facilitate the future discussion, we will now normalize the positions of these four sides.

We first ensure that the intersection $I(A', b)$ is directly adjacent to the two polygon vertices $I(a, b)$ and $I(A', B')$ in the arrangement of the four sides, as shown in Figure 7b. This can be achieved by swapping the labels a, A' with the labels b, B' if necessary, and by independently swapping the labels a', A' with b', B' if necessary. Our assumptions are invariant under these swaps.

By an affine transformation we may finally assume that $I(A', b)$ is the origin; b lies on the x -axis and is directed to the right; and A' lies on the y -axis and is directed upwards. Then a has a positive slope and its interior is in the upper half-plane, and B' has a positive slope and its interior is to the right of the y -axis, see Figure 7c.

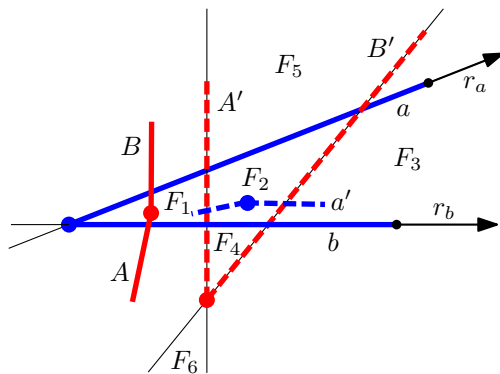


Figure 8 Case 1: $I(A, B) \in F_1, I(a', b') \in F_2$.

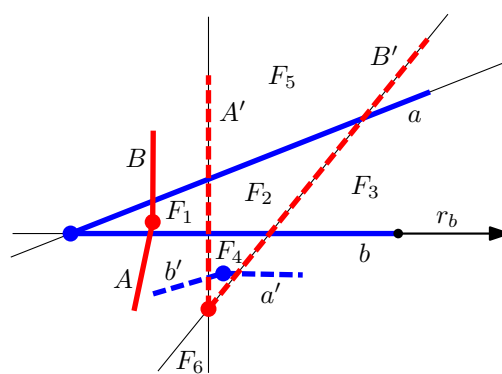


Figure 9 Case 2: $I(A, B) \in F_1, I(a', b') \in F_4$.

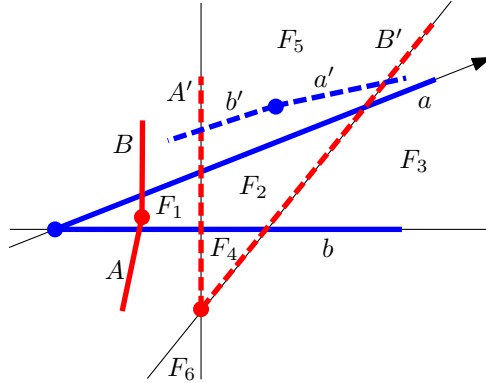
The arrangement of the lines through a, b, A', B' has 11 faces, some of which are marked as F_1, \dots, F_6 in Figure 7. Our current assumption is that both a, b and a', b' are hooking: The hooking of a, b means that $I(A, B) \in \text{Cone}(a, b) = F_1 \cup F_2 \cup F_3$. By the Axis Property (Observation 6), the line through $I(A', B')$ and $I(a', b')$ must separate A' from B' . Therefore, the vertex $I(a', b')$ can lie only in $F_2 \cup F_4 \cup F_5 \cup F_6$. Thus, based on the faces that contain $I(A, B)$ and $I(a', b')$, there are 12 cases to consider. Some of these cases are symmetric, and all can be easily dismissed, as follows.

In the figures, the four sides a', b', A', B' , which are associated to the second associated pair are dashed. All dashed sides of one polygon must intersect all solid sides of the other polygon.

1. $I(A, B) \in F_1$ and $I(a', b') \in F_2$, see Figure 8 (symmetric to $I(A, B) \in F_2$ and $I(a', b') \in F_4$). Let r_a (resp., r_b) be the ray on $\ell(a)$ (resp., $\ell(b)$) that goes from the right endpoint of a (resp., b) to the right. Since a' is not allowed to cross b , the only way for a' to intersect A is by crossing r_b . Similarly, in order to intersect B , a' has to cross r_a . However, it cannot intersect both r_a and r_b , by Observation 4.

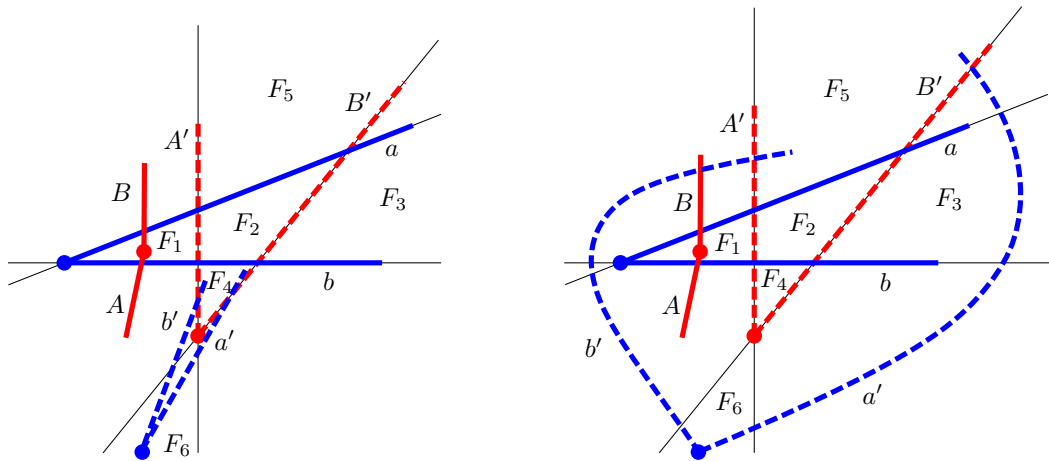
Since we did not use the assumption that A, B are hooked, the analysis holds for the symmetric Case 6, $I(A, B) \in F_2$ and $I(a', b') \in F_4$, as well.

2. $I(A, B) \in F_1$ and $I(a', b') \in F_4$, see Figure 9. Since a' is not allowed to cross b , the only way for a' to intersect B is by crossing r_b . However, in this case a' cannot intersect A .



■ **Figure 10** Case 3: $I(A, B) \in F_1$ and $I(a', b') \in F_5$.

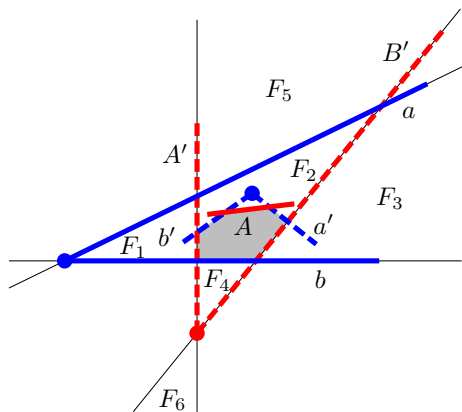
3. $I(A, B) \in F_1$ and $I(a', b') \in F_5$, see Figure 10 (symmetric to $I(A, B) \in F_3$ and $I(a', b') \in F_4$). Both a' and b' must intersect A , and they have to go below the line $\ell(b)$ to do so. However, a' can only cross $\ell(b)$ to the right of b , and b' can only cross $\ell(b)$ to the left of b , and therefore they cross A from different sides. This is impossible, because a' and b' start from the same point.
4. $I(A, B) \in F_1$ and $I(a', b') \in F_6$. If one of the polygon sides a' and b' has an endpoint in F_4 (see Figure 11a), then this side cannot intersect B . So assume otherwise, see Figure 11b. The side a' intersects B' and is disjoint from A' , while b' is disjoint from B' and intersects A' . (Due to space limitation some line segments are drawn schematically as curves.) Thus, each of a' and b' has an endpoint in $F_2 \cup F_5$. But then $I(A, B) \in \text{Cone}(a', b')$ and it follows from Observation 4 that neither A nor B can intersect both a' and b' .
5. $I(A, B) \in F_2$ and $I(a', b') \in F_2$, see Figure 12. Since a', b' is hooking, $I(A', B') \in \text{Cone}(a', b')$, and the line segments a', b', A', b, B' enclose a convex pentagon. The polygon side A must intersect b, a' and b' , but it is restricted to $F_2 \cup F_4$. It follows that A must intersect three sides of the pentagon, which is impossible. (This is in fact the only place where we need the assumption that a', b' is hooking.)
6. $I(A, B) \in F_2$ and $I(a', b') \in F_4$. This is symmetric to Case 1.
7. $I(A, B) \in F_2$ and $I(a', b') \in F_5$, see Figure 13 (symmetric to $I(A, B) \in F_3$ and $I(a', b') \in F_2$). Then A is restricted to $F_2 \cup F_4$, while a' and b' do not intersect F_2 and F_4 . Therefore A can intersect neither a' nor b' .
8. $I(A, B) \in F_2$ and $I(a', b') \in F_6$. This case is very similar to Case 4, where $I(A, B) \in F_1$ and $I(a', b') \in F_6$, see Figure 11. If one of the polygon sides a' and b' has an endpoint in F_4 , then it cannot intersect B . Otherwise, $I(A, B) \in \text{Cone}(a', b')$ and therefore, neither A nor B can intersect both a' and b' .
9. $I(A, B) \in F_3$ and $I(a', b') \in F_2$. This is symmetric to Case 7.



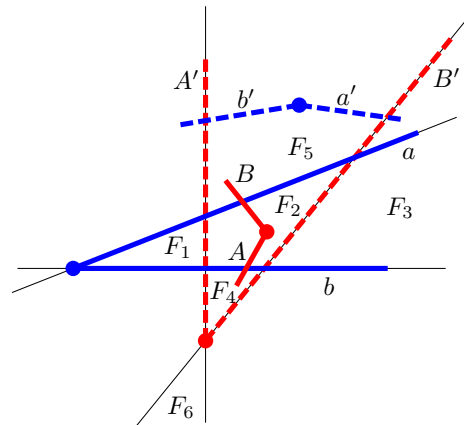
(a) At least one of the sides a' and b' has an endpoint in F_4 .

(b) None of the sides a' and b' has an endpoint in F_4 .

■ **Figure 11** Case 4: $I(A, B) \in F_1$ (or $I(A, B) \in F_2$, which is similar) and $I(a', b') \in F_6$.



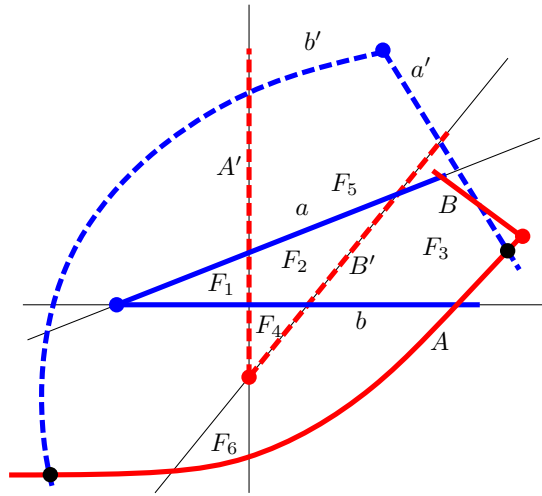
■ **Figure 12** Case 5: $I(A, B) \in F_2$, $I(a', b') \in F_2$.



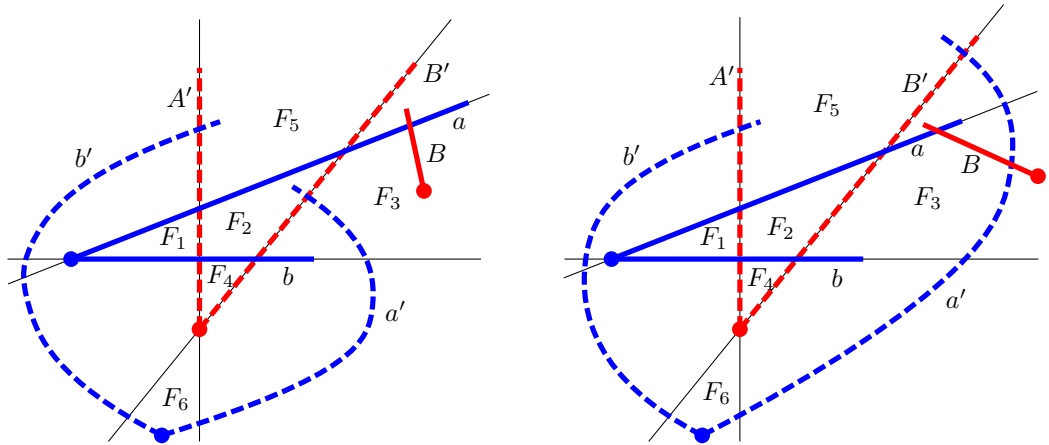
■ **Figure 13** Case 7: $I(A, B) \in F_2$, $I(a', b') \in F_5$.

- 10. $I(A, B) \in F_3$ and $I(a', b') \in F_4$. This is symmetric to Case 3.
- 11. $I(A, B) \in F_3$ and $I(a', b') \in F_5$, see Figure 14. Then the intersection of b' and A can lie only in the lower left quadrant. It follows that the triangle whose vertices are $I(a', b')$, $I(a', A)$ and $I(A, b')$ contains a and does not contain $I(A, B)$. This in turn implies that B cannot intersect both b' and a , without intersecting B' .
- 12. $I(A, B) \in F_3$ and $I(a', b') \in F_6$, see Figure 15. As in Case 4, we may assume that neither a' nor b' has an endpoint in F_4 , since then this side could not intersect B . We may also assume that $I(A, B) \notin \text{Cone}(a', b')$ for otherwise neither A nor B intersects both of a' and b' , according to Observation 4. If a' has an endpoint in F_2 , then it cannot intersect B (see Figure 15a). Otherwise, if a' has an endpoint in F_5 , then B cannot intersect b' (Figure 15b).

We have finished the case that a, b and a', b' are hooking. Suppose now that a, b and a', b' are hooked, with respect to some pairs A, B and A', B' . Then A, B is hooking with respect to a, b and A', B' is hooking with respect to a', b' . Recall that A, B, A' and B' belong to four different connected components. Hence, this case can be handled as above, after exchanging the capital letters with the small letters (i.e., exchanging P and Q). ◀



■ **Figure 14** Case 11: $I(A, B) \in F_3$ and $I(a', b') \in F_5$.



(a) If a' has an endpoint in F_2 , then it cannot intersect B .

(b) If a' has an endpoint in F_5 , then B cannot intersect b' .

■ **Figure 15** Case 12: $I(A, B) \in F_3$ and $I(a', b') \in F_6$.

6 A weaker bound

The principal structure lemma is already powerful enough to get an improvement over the previous best bound:

► **Lemma 8.** G^D has at most $(n + 5)/2$ connected components.

Proof. Partition the sides q_0, q_1, \dots, q_{n-1} of Q into $(n - 1)/2$ disjoint pairs q_{2i}, q_{2i+1} , discarding the last side q_{n-1} . Let H_+ denote the subset of these pairs that are hooked. Suppose first that this set contains some pair q_{2i_0}, q_{2i_0+1} of sides that are in two different connected components. Combining q_{2i_0}, q_{2i_0+1} with any of the remaining pairs q_{2i}, q_{2i+1} of H_+ , Lemma 7 tells us that the sides q_{2i} and q_{2i+1} must either belong to the same connected component, or one of them must belong to $CC(q_{2i_0})$ or $CC(q_{2i_0+1})$. In other words, each remaining pair contributes at most one “new” connected component, and it follows that the sides in H_+ belong to at most $|H_+| + 1$ connected components. This conclusion holds also in the case that H_+ contains no pair q_{2i_0}, q_{2i_0+1} of sides that are in different connected components.

The same argument works for the complementary subset H_- of pairs that are not hooked, but hooking. Along with $CC(q_{n-1})$ there are at most $(|H_+| + 1) + (|H_-| + 1) + 1 = (n - 1)/2 + 3 = (n + 5)/2$ components. ◀

Together with Observation 3, this already improves the previous bound $mn - (m + \lceil \frac{n}{6} \rceil)$ for a large range of parameters, namely when $m \geq n \geq 11$:

► **Proposition 9.** *Let P and Q be simple polygons with m and n sides, respectively, such that m and n are odd and $m \geq n \geq 3$. Then there are at most $mn - (m + \frac{n-5}{2})$ intersection points between P and Q .* ◀

7 Ramsey-theoretic tools

We recall some classic results. A tournament is a directed graph that contains between every pair of nodes x, y either the arc (x, y) or the arc (y, x) but not both. A tournament is *transitive* if for every three nodes x, y, z the existence of the arcs (x, y) and (y, z) implies the existence of the arc (x, z) . Equivalently, the nodes can be ordered on a line such that all arcs are in the same direction. The following is easy to prove by induction.

► **Lemma 10** (Erdős and Moser [3]). *Every tournament on a node set V contains a transitive sub-tournament on $1 + \lfloor \log_2 |V| \rfloor$ nodes.*

Proof. Choose $v \in V$ arbitrarily, and let $N \subseteq V - \{v\}$ with $|N| \geq (|V| - 1)/2$ be the set of in-neighbors of v or the set of out-neighbors of v , whichever is larger. Then v together with a transitive sub-tournament of N gives a transitive sub-tournament of size one larger. ◀

A set of points p_1, p_2, \dots, p_r in the plane sorted by x -coordinates (and with distinct x -coordinates) forms an r -cup (resp., r -cap) if p_i is below (resp., above) the line through p_{i-1} and p_{i+1} for every i with $1 < i < r$.

► **Theorem 11** (Erdős–Szekeres Theorem for caps and cups in point sets [4]). *For any two integers $r \geq 2$ and $s \geq 2$, the value $ES(r, s) := \binom{r+s-4}{r-2}$ fulfills the following statement:*

Suppose that P is a set of $ES(r, s) + 1$ points in the plane with distinct x -coordinates such that no three points of P lie on a line. Then P contains an r -cup or an s -cap.

Moreover, $ES(r, s)$ is the smallest value that fulfills the statement. ◀

A similar statement holds for lines by the standard point-line duality. A set of lines $\ell_1, \ell_2, \dots, \ell_r$ sorted by slope forms an r -cup (resp., r -cap) if ℓ_{i-1} and ℓ_{i+1} intersect below (resp., above) ℓ_i for every $1 < i < r$.

► **Theorem 12** (Erdős–Szekeres Theorem for lines). *For the numbers $ES(r, s)$ from Theorem 11, the following statement holds for any two integers $r \geq 2$ and $s \geq 2$:*

If L is a set of $ES(r, s) + 1$ non-vertical lines in the plane no two of which are parallel and no three of which intersect at a common point, then L contains an r -cup or an s -cap. ◀

► **Theorem 13** (Erdős–Szekeres Theorem for monotone subsequences [4]). *For any integer $r \geq 0$, a sequence of $r^2 + 1$ distinct numbers contains either an increasing subsequence of length $r + 1$ or a decreasing subsequence of length $r + 1$.* ◀

8 Proof of Theorem 1

8.1 Imposing more structure on the examples

Going back to the proof of Theorem 1, recall that in light of Observation 3 it is enough to prove that G^D , the disjointness graph of P and Q , has at most constantly many connected components. We will use the following constants: $C_6 := 6$; $C_5 := (C_6)^2 + 1 = 37$; $C_4 := ES(C_5, C_5) + 1 = \binom{70}{35} + 1 = 112,186,277,816,662,845,433 < 2^{70}$; $C_3 := 2^{C_4 - 1}$; $C_2 := C_3 + 5$; $C_1 := 8C_2$; $C := C_1 - 1 < 2^{2^{70}}$.

We claim that G^D has at most C connected components. Suppose that G^D has at least $C_1 = C + 1$ connected components, numbered as $1, 2, \dots, C_1$. For each connected component j , we find two consecutive sides q_{i_j}, q_{i_j+1} of Q such that $CC(q_{i_j}) = j$ and $CC(q_{i_j+1}) \neq j$. We call q_{i_j} the *primary* side and q_{i_j+1} the *companion* side of the pair. We take these C_1 consecutive pairs in their cyclic order along Q and remove every second pair. This ensures that the remaining $C_1/2$ pairs are disjoint in the sense that no side of Q belongs to two different pairs.

We apply Lemma 5 to each of the remaining $C_1/2$ pairs q_{i_j}, q_{i_j+1} and find an associated pair $p_{k_j}, p_{k_j\pm 1}$ such that $(q_{i_j}, p_{k_j}), (q_{i_j+1}, p_{k_j\pm 1}) \in E^D$. Therefore, $CC(q_{i_j}) = CC(p_{k_j})$ and $CC(q_{i_j+1}) = CC(p_{k_j\pm 1}) \neq CC(q_{i_j})$. Again, we call p_{k_j} the primary side and $p_{k_j\pm 1}$ the companion side. We delete half of the pairs $p_{k_j}, p_{k_j\pm 1}$ in cyclic order along P , along with their associated pairs from Q , and thus we ensure that the remaining $C_1/4$ pairs are disjoint also on P .

At least $C_1/8$ of the remaining pairs q_{i_j}, q_{i_j+1} are hooking or at least $C_1/8$ of them are hooked. We may assume that at least $C_2 = C_1/8$ of the pairs q_{i_j}, q_{i_j+1} are hooking with respect to their associated pair, $p_{k_j}, p_{k_j\pm 1}$, for otherwise, $p_{k_j}, p_{k_j\pm 1}$ is hooking with respect to q_{i_j}, q_{i_j+1} and we may switch the roles of P and Q . Let us denote by Q_2 the set of C_2 hooking consecutive pairs $(q_{i_j}, q_{i_j\pm 1})$ at which we have arrived. (Because of the potential switch, we have to denote the companion side by $q_{i_j\pm 1}$ instead of q_{i_j+1} from now on.)

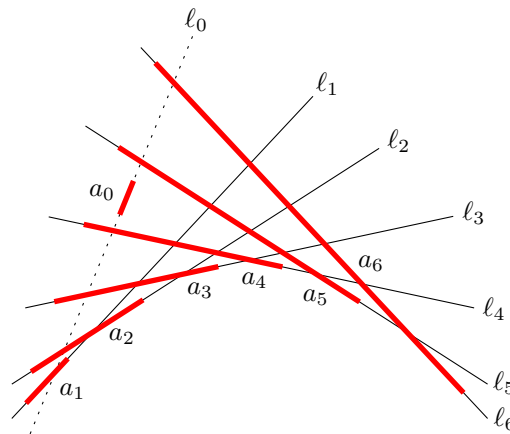
By construction, all C_2 primary sides q_{i_j} of these pairs belong to distinct components. We now argue that all C_2 adjacent companion sides $q_{i_j\pm 1}$ with at most one exception lie in the same connected component, provided that $C_2 \geq 4$.

We model the problem by a graph whose nodes are the connected components of G^D . For each pair $q_{i_j}, q_{i_j\pm 1}$, we insert an edge between $CC(q_{i_j})$ and $CC(q_{i_j\pm 1})$. The result is a multi-graph with C_2 edges and without loops. Two disjoint edges would represent two consecutive pairs of the form $(q_{i_j}, q_{i_j\pm 1})$ whose four sides are in four distinct connected components, but this is a contradiction to Lemma 7. Thus, the graph has no two disjoint edges, and such graphs are easily classified: they are the triangle (cycle on three vertices) and the star graphs K_{1t} , possibly with multiple edges. Overall, the graph involves at least $C_2 \geq 4$ distinct connected components $CC(q_{i_j})$, and therefore the triangle graph is excluded. Let v be the central vertex of the star. There can be at most one j with $CC(q_{i_j}) = v$, and we discard it. All other sides q_{i_j} have $CC(q_{i_j}) \neq v$, and therefore $CC(q_{i_j\pm 1})$ must be the other endpoint of the edge, that is, v .

In summary, we have found $C_2 - 1$ adjacent pairs $q_{i_j}, q_{i_j\pm 1}$ with the following properties.

- The primary sides q_{i_j} belong to $C_2 - 1$ distinct components.
- All companion sides $q_{i_j\pm 1}$ belong to the same component, distinct from the other $C_2 - 1$ components.
- All $2C_2 - 2$ sides of the pairs $q_{i_j}, q_{i_j\pm 1}$ are distinct.
- Each $q_{i_j}, q_{i_j\pm 1}$ is hooking with respect to an associated pair $p_{k_j}, p_{k_j\pm 1}$.
- All $2C_2 - 2$ sides of the pairs $p_{k_j}, p_{k_j\pm 1}$ are distinct.

Let us denote by Q'_2 the set of $C_2 - 1$ sides q_{i_j} .



■ **Figure 16** The seven sides a_0, a_1, \dots, a_6 . The lines l_0, \dots, l_6 form a 7-cup.

► **Proposition 14.** *There are no six distinct sides $q_a, q_b, q_c, q_d, q_e, q_f$ among the $C_2 - 1$ sides $q_{i_j} \in Q'_2$ such that q_a, q_b are avoiding or consecutive, q_c, q_d are avoiding or consecutive, and q_e, q_f are avoiding or consecutive.*

Proof. Suppose for contradiction that six such sides exist. It follows from Lemma 5 that there are two consecutive sides $p_{a'}$ and $p_{b'}$ of P such that $CC(p_{a'}) = CC(q_a)$ and $CC(p_{b'}) = CC(q_b)$.

Similarly, we find a pair of consecutive sides $p_{c'}$ and $p_{d'}$ of P such that $CC(p_{c'}) = CC(q_c)$ and $CC(p_{d'}) = CC(q_d)$, and the same story for e and f . By the pigeonhole principle, two of the three consecutive pairs $(p_{a'}, p_{b'})$, $(p_{c'}, p_{d'})$, $(p_{e'}, p_{f'})$ are hooking or two of them are hooked. This contradicts Lemma 7. ◀

Define a complete graph whose nodes are the $C_2 - 1$ sides $q_{i_j} \in Q'_2$, and color an edge (q_{i_j}, q_{i_k}) red if q_{i_j} and q_{i_k} are avoiding or consecutive and blue otherwise. Proposition 14 says that this graph contains no red matching of size three. This means that we can get rid of all red edges by removing at most 4 nodes. To see this, pick any red edge and remove its two nodes from the graph. If any red edge remains, remove its two nodes. Then all red edges are gone, because otherwise we would find a matching with three red edges.

We conclude that there is a blue clique of size $C_3 = C_2 - 5$, i.e., there is a set $Q_3 \subset Q'_2$ of C_3 polygon sides among the $C_2 - 1$ sides $q_{i_j} \in Q'_2$ that are pairwise non-avoiding and disjoint, i.e., they do not share a common endpoint.

Our next goal is to find a subset of 7 segments in Q_3 that are arranged as in Figure 16. To define this precisely, we say for two segments s and s' that s *stabs* s' if $I(s, s') \in s'$, see Figure 4. Among any two non-avoiding and non-consecutive sides s and s' , either s stabs s' or s' stabs s , but not both. Define a tournament T whose nodes are the C_3 sides $q_{i_j} \in Q_3$, and the arc between each pair of nodes is oriented towards the stabbed side. It follows from Lemma 10 that T has a transitive sub-tournament of size $1 + \lceil \log_2 C_3 \rceil = C_4$.

Furthermore, since $C_4 = ES(C_5, C_5) + 1$, it follows from Theorem 12 that there is a subset of C_5 sides such that the lines through them form a C_5 -cup or a C_5 -cap. By a vertical reflection if needed, we may assume that they form a C_5 -cup.

We now reorder these C_5 sides q_{i_j} of Q in stabbing order, according to the transitive sub-tournament mentioned above. By the Erdős–Szekeres Theorem on monotone subsequences (Theorem 13), there is a subsequence of size $C_6 + 1 = \sqrt{C_5 - 1} + 1 = 7$ such that their slopes form a monotone sequence. By a horizontal reflection if needed, we may assume that they have decreasing slopes.

1:14 The Number of Intersections Between Two Simple Polygons

We rename these 7 segments to a_0, a_1, \dots, a_6 , and we denote the line $\ell(a_i)$ by ℓ_i , see Figure 16. We have achieved the following properties:

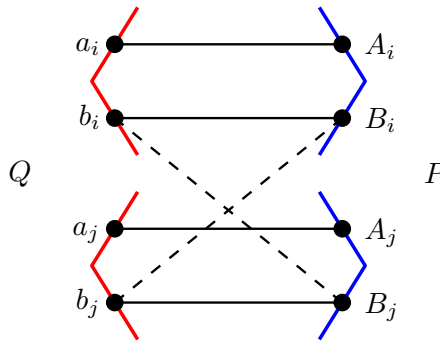
- The lines ℓ_0, \dots, ℓ_6 form a 7-cup, with decreasing slopes in this order.
- The segments a_i are pairwise disjoint and non-avoiding.
- a_i stabs a_j for every $i < j$.

These properties allow a_0 to lie between any two consecutive intersections on ℓ_0 . There is no such flexibility for the other sides: Every side a_j is stabbed by every preceding side a_i . For $1 \leq i < j$, a_i cannot stab a_j from the right, because then a_0 would not be able to stab a_i . Hence, the arrangement of the sides a_1, \dots, a_6 must be exactly as shown in Figure 16, in the sense that the order of endpoints and intersection points along each line ℓ_i is fixed. We will ignore a_0 from now on.

8.2 Finalizing the analysis

Recall that every a_i is the primary side of two consecutive sides a_i, b_i of Q that are hooking with respect to an associated pair A_i, B_i of consecutive sides of P . The sides a_i and A_i are the primary sides and b_i and B_i are the companion sides. All these 4×6 sides are distinct, and they intersect as follows: a_i intersects B_i and is disjoint from A_i ; b_i intersects A_i and is disjoint from B_i ; and $I(A_i, B_i) \in \text{Cone}(a_i, b_i)$.

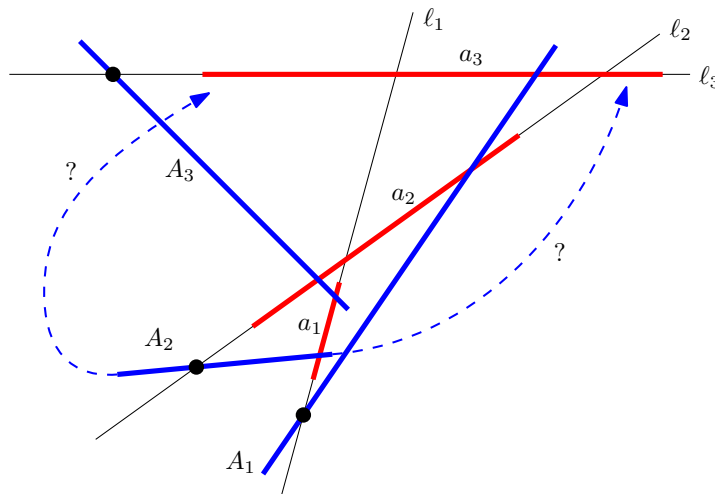
Figure 17 summarizes the intersection pattern among these sides. A side A_i must intersect every side a_j with $j \neq i$ and every side b_j since $\text{CC}(A_i) = \text{CC}(a_i) \neq \text{CC}(a_j)$ and $\text{CC}(A_i) = \text{CC}(a_i) \neq \text{CC}(b_i) = \text{CC}(b_j)$. (Recall that all companion sides b_i belong to the same component.) Similarly, every side B_i must intersect every side a_j . We have no information about the intersection between B_i and b_j , as these sides belong to the same connected component.



■ **Figure 17** The subgraph of G^D induced on two pairs of consecutive sides a_i, b_i and a_j, b_j of P and their associated partner pairs A_i, B_i and A_j, B_j of Q . Parts of P and Q are shown to indicate consecutive sides. The dashed edges may or may not be present.

We will now derive a contradiction through a series of case distinctions.

Case 1: There are three segments A_i with the property that A_i crosses ℓ_i to the left of a_i . Without loss of generality, assume that these segments are A_1, A_2, A_3 , see Figure 18. The segments A_1, A_2, A_3 must not cross because P is a simple polygon. Therefore A_1 intersects a_2 to the right of $I(a_1, a_2)$ because otherwise A_1 would cross A_2 on the way between its intersections with ℓ_2 and with a_1 . A_3 must cross ℓ_3, a_2, a_1 in this order, as shown. But then A_1 and A_3 (and a_2) block A_2 from intersecting a_3 .



■ **Figure 18** The assumed intersection points between A_i and ℓ_i are marked.

Case 2: There at most two segments A_i with the property that A_i crosses ℓ_i to the left of a_i . In this case, we simply discard these segments. We select four of the remaining segments and renumber them from 1 to 4.

From now on, we can make the following assumption:

General Assumption: For every $1 \leq i \leq 4$, the segment A_i does not cross ℓ_i at all, or it crosses ℓ_i to the right of a_i .

This implies that A_3 must intersect the sides a_2, a_1, a_4 in this order, and it is determined in which cell of the arrangement of the lines $\ell_1, \ell_2, \ell_3, \ell_4$ the left endpoint of A_3 lies (see Figures 16 and 19). For the right endpoint, we have a choice of two cells, depending on whether A_3 intersects ℓ_3 or not.

We denote by $\text{left}(s)$ and $\text{right}(s)$ the left and right endpoints of a segment s . We distinguish four cases, based on whether the common endpoint of A_3 and B_3 lies at $\text{left}(A_3)$ or $\text{right}(A_3)$, and whether the common endpoint of a_3 and b_3 lies at $\text{left}(a_3)$ or $\text{right}(a_3)$.

Case 2.1: $I(A_3, B_3) = \text{left}(A_3)$ and $I(a_3, b_3) = \text{right}(a_3)$, see Figure 19.

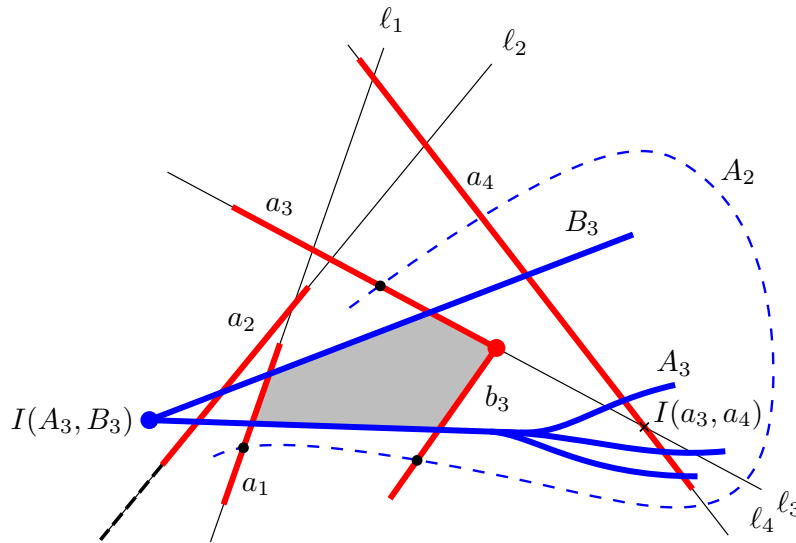
As indicated in the figure, we leave it open whether and where A_3 intersects ℓ_3 . We know that b_3 must lie below ℓ_3 because $I(A_3, B_3) \in \text{Cone}(a_3, b_3)$.

We claim that A_2 cannot have the required intersections with a_1, a_3 , and b_3 . Let us first consider a_1 : It is cut into three pieces by A_3 and B_3 .

If A_2 intersects the middle piece of a_1 in the wedge between A_3 and B_3 , then A_2 intersects exactly one of a_3 and b_3 inside the wedge, as these parts together with a_1 are three sides of a convex pentagon. If A_2 intersects a_3 , then it has crossed ℓ_3 and it cannot cross b_3 thereafter. If A_2 intersects b_3 , it must cross ℓ_4 before leaving the wedge, and then it cannot cross a_3 thereafter.

Suppose now that A_2 crosses the bottom piece of a_1 . Then it cannot go around A_3, B_3 to the right in order to reach a_3 because it would have to intersect ℓ_4 twice. A_2 also cannot pass to the left of A_3, B_3 because it cannot cross ℓ_2 through a_2 or, by the general assumption, to the left of a_2 .

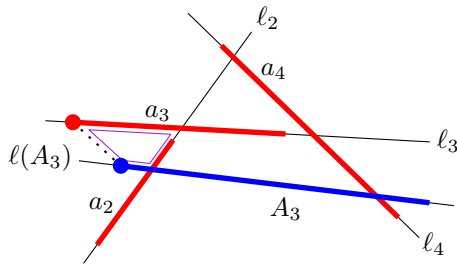
Suppose finally that A_2 crosses the top piece of a_1 . Then it would have to cross ℓ_3 twice before reaching b_3 .



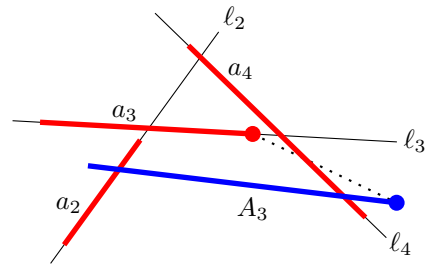
■ **Figure 19** Case 2.1, $I(A_3, B_3) = \text{left}(A_3)$ and $I(a_3, b_3) = \text{right}(a_3)$. A hypothetical segment A_2 is shown as a dashed curve. The side a_2 and the part of ℓ_2 to the left of a_2 is blocked for A_2 .

Case 2.2: $I(A_3, B_3) = \text{left}(A_3)$ and $I(a_3, b_3) = \text{left}(a_3)$.

If $\ell(A_3)$ does not intersect a_3 , we derive a contradiction as follows, see Figure 20. We know that the sides a_2, a_3, a_4 must be arranged as shown. The segment A_3 crosses a_2 but not a_3 . Now, the parts of a_3 and A_3 to the left of ℓ_2 form two opposite sides of a quadrilateral, as shown in the figure. If this quadrilateral were not convex, then either $\ell(A_3)$ would intersect a_3 , which we have excluded by assumption, or ℓ_3 would intersect A_3 left of a_3 , contradicting the General Assumption. Thus, the sides a_3 and A_3 violate the Axis Property (Observation 6), which requires a_3 and A_3 to lie on different sides of the line through $I(A_3, B_3)$ and $I(a_3, b_3)$.



■ **Figure 20** Case 2.2. $I(A_3, B_3) = \text{left}(A_3)$, $I(a_3, b_3) = \text{left}(a_3)$, $\ell(A_3)$ does not intersect a_3 .

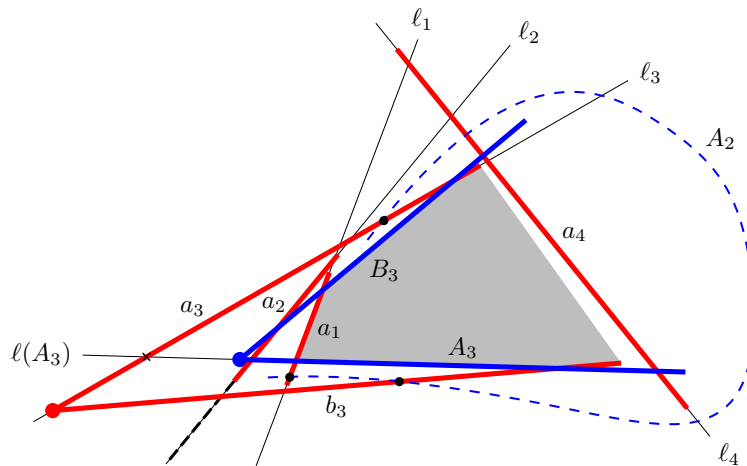


■ **Figure 21** Case 2.3. $I(A_3, B_3) = \text{right}(A_3)$, and $I(a_3, b_3) = \text{right}(a_3)$, A_3 lies below ℓ_3 .

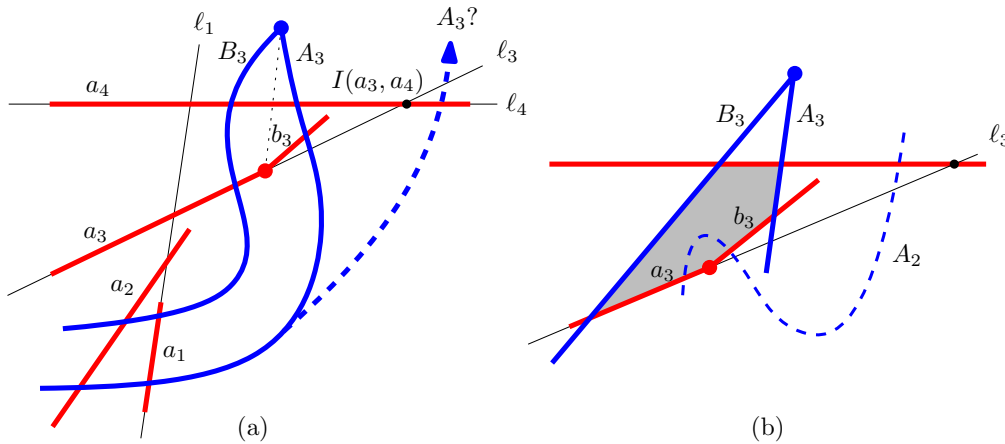
If $\ell(A_3)$ intersects a_3 , the situation must be as shown in Figure 22: the pair A_3, B_3 is hooked by a_3 and b_3 . The analysis of Case 2.1 (Figure 19) applies verbatim, except that the word “pentagon” must be replaced by “hexagon”.

Case 2.3: $I(A_3, B_3) = \text{right}(A_3)$, and $I(a_3, b_3) = \text{right}(a_3)$.

If A_3 lies entirely below ℓ_3 , then A_3 together with a_3 violates the Axis Property (Observation 6), see Figure 21. Let us therefore assume that A_3 intersects ℓ_3 (to the right of a_3), and thus $\text{right}(A_3) = I(A_3, B_3)$ lies above ℓ_3 , see Figure 23a. Then b_3 must also lie above ℓ_3 , because a_3, b_3 is supposed to be hooking, that is, $I(A_3, B_3) \in \text{Cone}(a_3, b_3)$.



■ **Figure 22** Case 2.2, $I(A_3, B_3) = \text{left}(A_3)$, $I(a_3, b_3) = \text{left}(a_3)$, and $\ell(A_3)$ intersects A_3 . A hypothetical segment A_2 is shown as a dashed curve.



■ **Figure 23** Case 2.3. A_3 intersects ℓ_3 .

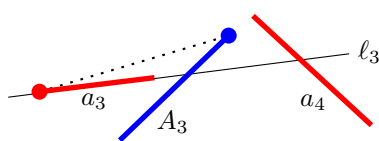
It follows that A_3 cannot intersect ℓ_3 to the right of $I(a_3, a_4)$ (the option shown as a dashed curve), because otherwise it would miss b_3 : b_3 is blocked by a_4 . Thus, the situation looks like in Figure 23a. Figure 23b shows the position of the relevant pieces. The segments a_4, B_3, a_3, b_3, A_3 enclose a convex pentagon. Now, the segment A_2 should intersect a_3, b_3 , and a_4 without crossing A_3 and B_3 , like the dashed curve in the figure. This is impossible.

Case 2.4: $I(A_3, B_3) = \text{right}(A_3)$ and $I(a_3, b_3) = \text{left}(a_3)$.

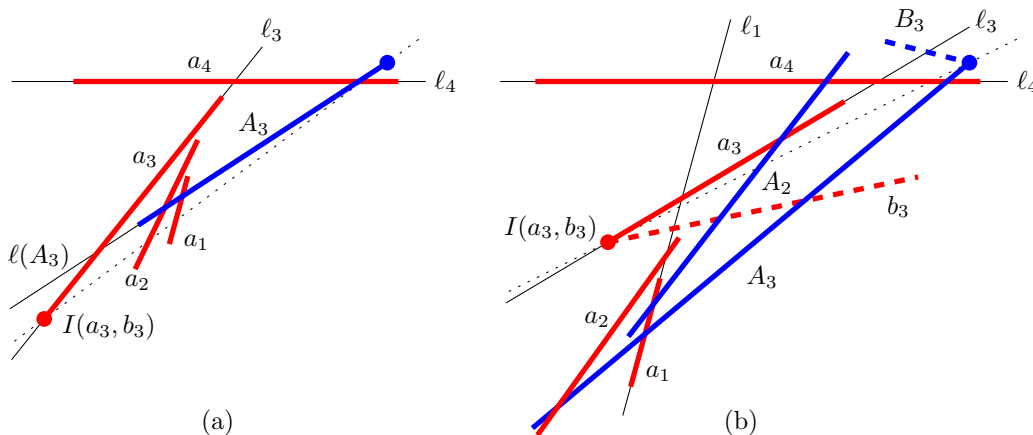
If A_3 intersects ℓ_3 (to the right of a_3), then A_3 together with a_3 violates the Axis Property (Observation 6), see Figure 24. We thus assume that A_3 lies entirely below ℓ_3 .

If $\ell(A_3)$ passes above $I(a_3, b_3) = \text{left}(a_3)$, the sides a_3 and A_3 violate the Axis Property see Figure 25a. On the other hand, if $\ell(A_3)$ passes below $I(a_3, b_3) = \text{left}(a_3)$, as shown in Figure 25b, then b_3 must cross ℓ_1 to the right of a_1 in order to reach A_2 . Again by the Axis Property, B_3 must remain above the dotted axis line through $I(A_3, B_3) = \text{right}(A_3)$ and $I(a_3, b_3) = \text{left}(a_3)$. On ℓ_1 , b_3 separates a_1 from the axis line, and hence a_1 lies below the axis line. Therefore B_3 and a_1 cannot intersect.

This concludes the proof of Theorem 1. ◀



■ **Figure 24** Case 2.4. A_3 intersects ℓ_3 .



■ **Figure 25** Case 2.4. A_3 lies below ℓ_3 .

References

- 1 J. Černý, J. Kára, D. Král', P. Podbrský, M. Sotáková, and R. Šámal. On the number of intersections of two polygons. *Comment. Math. Univ. Carolinae*, 44(2):217–228, 2003. URL: <https://cmuc.karlin.mff.cuni.cz/cmuc0302/cmuc0302.htm>.
- 2 Michael B. Dillencourt, David M. Mount, and Alan Saalfeld. On the maximum number of intersections of two polyhedra in 2 and 3 dimensions. In *Proceedings of the 5th Canadian Conference on Computational Geometry, Waterloo, Ontario, Canada, August 1993*, pages 49–54. University of Waterloo, 1993.
- 3 P. Erdős and L. Moser. On the representation of directed graphs as unions of orderings. *Magyar Tud. Akad. Mat. Kutató Int. Közl.*, 9:125–132, 1964.
- 4 P. Erdős and G. Szekeres. A combinatorial problem in geometry. *Compositio Mathematica*, 2:463–470, 1935.
- 5 Felix Günther. The maximum number of intersections of two polygons, July 2012. withdrawn by the author. [arXiv:1207.0996](https://arxiv.org/abs/1207.0996).